SVU-International Journal of Engineering Sciences and Applications (2024) 5(1): 89-98
Print ISSN 2785-9967 | Online ISSN 2735-4571
DOI 10.21608/svusrc.2023.240888.1153

Optimizing Grid-Dependent Hybrid Renewable Energy System with the African Vultures Optimization Algorithm

Montaser Abdelsattar[1,*], Abdelgayed Mesalam[2], Abdelrahman Fawzi[3], and I. Hamdan[4]

Abstract Countries aiming to achieve their sustainable development goals recognize the significance of adopting hybrid power systems to ensure access to clean, dependable, and cost-effective energy. In this study, an african vultures optimization algorithm (AVOA) is introduced for the efficient design of a grid-tied hybrid renewable energy (HRE) system that incorporates wind turbines, photovoltaic (PV) panels, and energy storage through batteries. The system is meticulously designed to ensure the provision of clean, dependable, and cost-effective energy through the utilization of HRE systems. Because of the complex and non-linearity of the sizing problem, AVOA, being an efficient metaheuristic approach, presents a promising solution. An empirical case study is presented, focusing on an HRE system introduced in the Zafarana region of Egypt. This case study serves as an evaluation of the effectiveness of the proposed optimizer. This study will provide valuable insights for decision-makers in Egypt, offering a practical solution to enhance the integration of intermittent renewable systems and ensure a continuous and reliable energy supply. The results achieved through AVOA are compared with those obtained using the particle swarm optimization (PSO) algorithm for evaluation. Simulation results validate the superior of the AVOA over the PSO, showing its potential to deliver promising results.

Keywords: Hybrid renewable energy system; Cost of energy; Carbon emissions; Loss of power supply probability; African vultures optimization algorithm.

1 Introduction

In recent times, fossil fuels have been the primary energy source in many regions globally. Nonetheless, these fossil fuels can be depleted and often have detrimental environmental effects during their conversion into usable energy forms [1], [2]. Considering the disadvantages associated with the use of fossil fuels for energy purposes, there is an immediate requirement to identify cost-effective, dependable, and environmentally friendly alternative energy sources. Renewable systems like photovoltaics (PV), wind turbines (WTs), and hydropower represent highly appealing options for clean energy generation, particularly in small-scale and remote regions [3], [4].

Due to the natural fluctuations of solar and wind energy sources, relying solely on one energy source often necessitates a large and expensive generation and storage system. To mitigate this, hybrid solar-wind systems are commonly employed, combining the benefits of both technologies to deliver a more dependable and cost-effective power supply, particularly in remote regions [5]. Energy storage technologies, including batteries, supercapacitors, fuel cells, molten salt, flywheels, compressed air, and hydroelectric pumped storage, offer viable solutions to address the intermittency of renewable systems.

Designing economically and reliably efficient hybrid renewable energy (HRE) systems poses challenges due to the intermittency of sources like solar radiation and wind speed. The primary objective is to achieve an optimal and dependable power supply configuration while managing component costs effectively [6]. In the literature, numerous research articles are presenting various techniques and algorithms for an optimum size of HRE systems [7]–[12].

Three optimization techniques, namely cuckoo search (CS), genetic algorithms, and particle swarm optimization (PSO), were employed in Ref. [13] to determine the optimal setup of a standalone HRE system incorporating PV, WT, battery, and diesel. The outcomes revealed that

Received: 5 October 2023/ Accepted: 4 November 2023
*Corresponding Author: Montaser Abdelsattar, Montaser.A.Elsattar@eng.svu.edu.eg
Other Author: Abdelgayed Mesalam, abdgyd2012@hotmail.com, Abdelrahman Fawzi, abdrahmanfawazy@eng.svu.edu.eg, I. Hamdan, Ibrahimhamdan86@eng.svu.edu.eg
1,2,3,4. Electrical Engineering Department, Faculty of Engineering, South Valley University, Qena 83523, Egypt

CS outperformed other methods in terms of both accuracy and the time needed to obtain the optimal sizing. In Ref. [14], PSO has been applied to obtain a minimum total investment cost at the lowest loss of load probability of a grid-tied HRE system containing PV and WT. PSO was applied in Ref. [15] to optimize the design of an independent HRE system comprising PV, WT, and diesel with energy storage. The simulation outcomes confirmed PSO's potential as an optimization method, as it consistently reached the global optimum. In Ref. [16], a new proposed program was created to manage the sizing and optimization of HRE system, encompassing PV, WT, battery, and diesel, while segregating the load into high and low-priority categories. The simulation results validated that this load segmentation strategy decreased system size and enhanced system reliability.

The primary contribution of this research article can be summarized as:

- The African vultures optimization algorithm (AVOA) has been used to optimize the size of a grid-connected HRE system and compare its results with those obtained using PSO.
- A real case study was chosen in Egypt to validate the proposed optimization approach.
- Three terms make up the objective function: cost of energy (COE), carbon emissions, and loss of power supply probability (LPSP).

The paper is structured as follows: In Section 2, a brief overview of the construction of the proposed HRE system is provided. Section 3 illustrates the operational strategy. Section 4 covers the problem statement of optimization and introduces AVOA. Section 5 presents a summary of simulation results and discussions. Lastly, in Section 6, the conclusion is presented.

2 Overview of the Proposed HRE System's Construction

The proposed system consists of five primary components, alongside the AC and DC buses. These components encompass WTs, PV panels, batteries, converters, and an external grid. Figure 1 depicts a simplified single-line diagram of the suggested grid-tied HRE system.

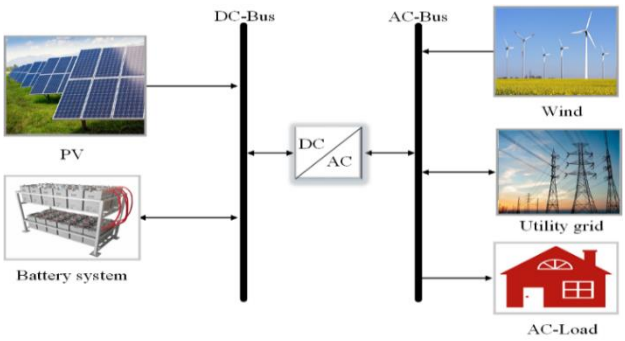

Fig. 1. Single line diagram of the grid-tied proposed HRE system.

2.1 PV panels

The output power ($P_{PVS}(t)$) produced by a PV system (PVS) can be described using the following equations, taking into account the irradiance ($r(t)$) and the ambient temperature ($T_{amb}(t)$) [17].

$$P_{PVS}(t) = n_{PV,Panels} \times P_{R,PV} \times \frac{r(t)}{r_{nom}} \times (1 - \sigma_T(T_{Cell}(t) - T_{nom})) \quad (1)$$

$$T_{Cell}(t) = T_{amb}(t) + 0.034 \times r(t) \quad (2)$$

where, the variables $n_{PV,Panels}$, $P_{R,PV}$, r_{nom}, T_{nom}, and σ_T correspond to the following: the number of PV panels, the rated power of each PV panel, the intensity of solar radiation, the cell temperature under standard conditions, and the temperature coefficient of power of the chosen PV panel, respectively.

2.2 Wind turbines

Considering the fundamental principles of wind energy, the anticipated energy produced by a wind turbine ($P_{WT}(t)$) can be expressed in the following manner [18]:

$$P_{WT}(t) = \begin{cases} n_{WTs} \cdot P_{R,WT} \cdot \frac{w^2(t) - w_{c,i}^2}{w_R^2 - w_{c,i}^2}, & w_{c,i} < w(t) < w_R \\ n_{WTs} \cdot P_{R,WT}, & w_R < w(t) < w_{c,o} \\ 0, & w(t) < w_{c,i} \text{ and } w(t) > w_{c,o} \end{cases} \quad (3)$$

where, n_{WTs}, $P_{R,WT}$, $w(t)$, w_R, $w_{c,i}$, and $w_{c,o}$ correspond to the following: the number of WTs, each WT's rated power, wind speed at time t, WT's rated wind speed, cut-in, and cut-off wind speed, respectively.

2.3 Batteries

The energy storage system is essential in maintaining a consistent power supply to the desired load due to the unpredictable nature of wind speed and solar radiation. It helps to store excess energy during periods of high generation and release it during times of low generation, ensuring a continuous flow of power. The state of charge (SOC) of batteries can be determined by continuously monitoring the energy being charged into and discharged from the battery banks. The calculation for the battery SOC at any given time is as follows [19]:

$$SOC(t) = SOC(t-1)(1-\mu_B) + \left[P_{PVS}(t) + \frac{P_{WT}(t)-P_L(t)}{\eta_{conv}}\right]\cdot \eta_C \quad \text{(charging periods)} \tag{4}$$

$$SOC(t) = SOC(t-1)(1-\mu_B) - \left[\frac{P_L(t)-P_{WT}(t)}{\eta_{conv}} - P_{PVS}(t)\right]\cdot \eta_D \quad \text{(discharging periods)} \tag{5}$$

where, $SOC(t)$ and $SOC(t-1)$ are batteries' SOC at time t and $t-1$, respectively, $P_L(t)$ is load demand for energy, μ_B denotes self-discharge rate, η_{conv} is converter efficiency. In addition η_C and η_D signify the charging and discharging efficiencies of the battery, respectively.

2.4 External grid

In situations where the batteries are unable to meet the load demand, the external grid serves as a backup, supplying the required electricity ($P_{Deficit}(t)$). The calculation for the purchased power from the grid ($P_{GP}(t)$) is determined by **Eq. (6)**. Conversely, during times of excess electricity and when the batteries are completely charged, any excess energy ($P_{Surplus}(t)$) is fed back into the utility grid, and the calculation for the sold power to the grid ($P_{GS}(t)$) is described in **Eq. (7)** [20].

$$P_{GP}(t) = \begin{cases} P_{Deficit}(t), & P_{Deficit}(t) < P_{GP}(Max) \\ P_{GP}(Max), & else \end{cases} \tag{6}$$

$$P_{GS}(t) = \begin{cases} P_{Surplus}(t), & P_{Surplus}(t) < P_{GS}(Max) \\ P_{GS}(Max), & else \end{cases} \tag{7}$$

where, $P_{GP}(Max)$ and $P_{GS}(Max)$ denote the maximum amount of power that can be obtained from the grid and the maximum amount of excess energy that can be supplied back to the grid, respectively.

2.5 Converter

The inverter plays a crucial role in the system by converting the direct current (DC) power generated by the PVS and batteries into alternating current (AC) power to meet the load demand. Any excess power is then supplied to the grid. Additionally, during periods of high generation, the inverter is responsible for converting the AC power generated by WTs into DC power to recharge the batteries. The rated power of the converter ($P_{R,conv}(t)$) has been chosen based on the peak load ($P_{L,peak}$) using the following formula [21].

$$P_{R,conv}(t) = P_{L,peak} \cdot SF \tag{8}$$

where, SF represents the safety factor, and it is recommended to have a converter's rated power that is 25% to 30% higher than the peak load.

3 Operation Strategy

The functioning of the suggested HRE system is outlined in the subsequent operational scenarios.

If the power generated from renewable systems is equal to the power required by the load, then the entire renewable power generated is supplied to the load. This scenario ensures maximum utilization of renewable energy and minimizes the need for backup power sources or reliance on non-renewable energy.

If the generation exceeds the load requirements, the surplus power is directed towards charging the batteries. If there is still excess energy beyond the battery capacity, it is fed into the electric grid. Any remaining surplus energy over $P_{GS}(Max)$ is utilized by a dump load.

During periods of low generation, the batteries are utilized to meet the deficit in load demand. If the required power to cover the load exceeds the energy stored in the batteries, the electric grid provides the additional power needed to bridge the deficit. Any remaining deficit energy beyond the $P_{GP}(Max)$ is used in the calculation of LPSP.

A flowchart depicting the operation of the proposed HRE system can be observed in Fig. 2.

4 Optimization Problem

4.1 Cost of energy

The HRE system's cost of energy (COE), in ($/kWh), is determined by the following formula:

$$COE = \frac{C_{A,T}}{\sum_{t=1}^{8760} P_L(t)} \tag{9}$$

The total yearly cost of the HRE system ($C_{A,T}$) is computed by summing the individual costs of all system.

$$C_{A,T} = C_{A,I} + C_{A,R} + C_{A,O\&M} + C_{A,GP} - C_{A,GS} \tag{10}$$

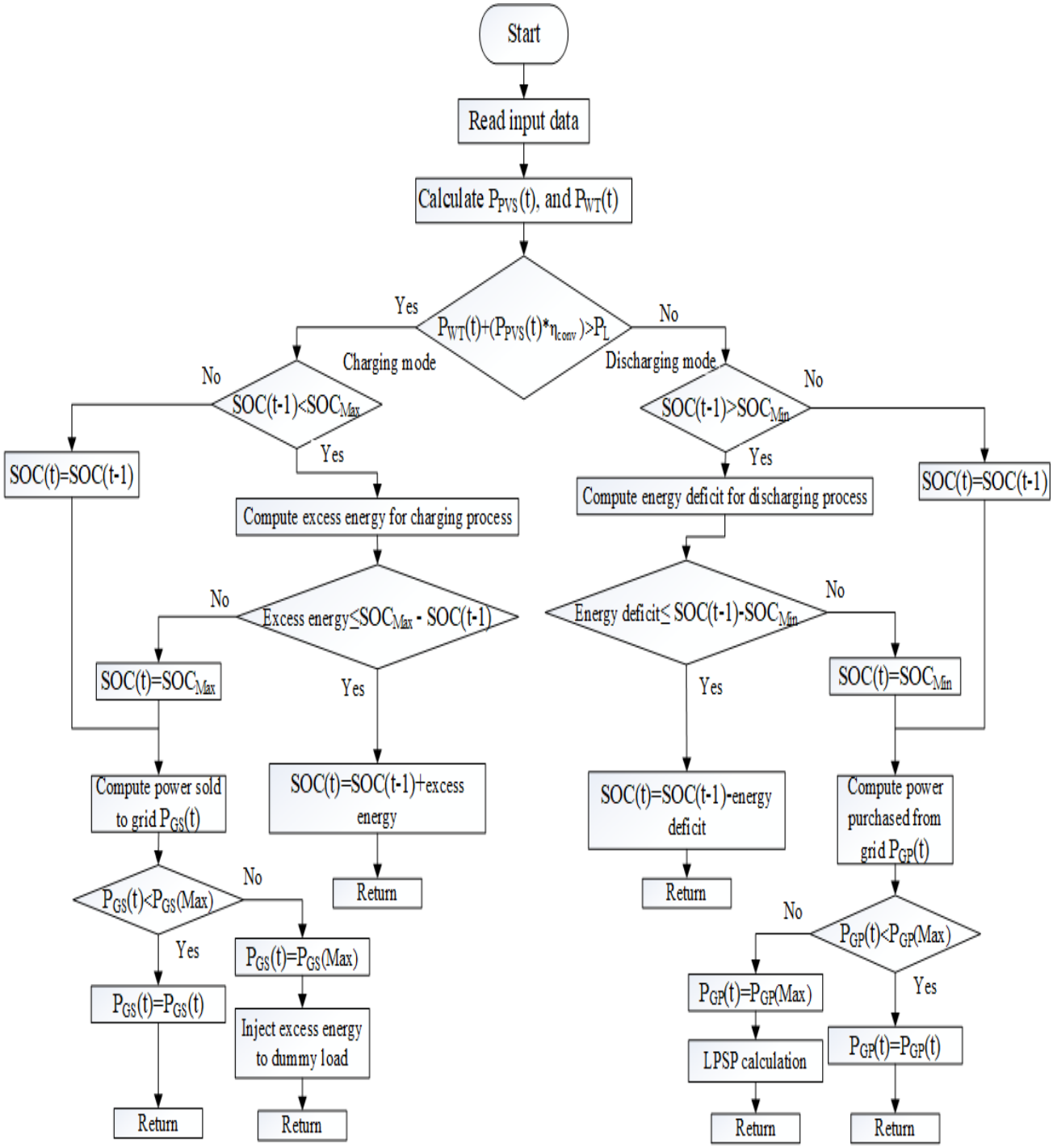

Fig. 2. Flowchart of strategies for power management.

where, $C_{A,I}$, $C_{A,R}$, $C_{A,O\&M}$, $C_{A,GP}$, and $C_{A,GS}$ denote the yearly costs of initial replacement, maintenance, purchased from the grid, and sold to the grid. Respectively. The yearly interest on the initial cost of each system component i, is calculated as follows [22]:

$$C_{A,C}^{i} = C_{C}^{i} \cdot CRF(r, m_i) \quad (11)$$

where i represents each component in HRE system, containing PVS, WTs, batteries, and the bi-directional converter. CRF, r, and m_i denote the capital recovery factor, rate of interest, and lifespan of each component, respectively.

The annual costs of purchased electricity from the grid and sold electricity to the grid can be computed by **Eqs. (12), and (13)** [23].

$$C_{A,GP} = C_P \sum_{t=1}^{8760} P_{GP}(t) \quad (12)$$

$$C_{A,GS} = C_S \sum_{t=1}^{8760} P_{GS}(t) \quad (13)$$

In this context, the cost of purchasing one kWh of electricity from the electric grid is denoted as C_P, with a specific value of \$0.08/kWh. On the other hand, the cost of supplying one kWh of electricity to the utility grid is represented as C_S, with a value of \$0.2/kWh [24].

The net present cost (NPC) of the HRE system is computed as follow [25]:

$$NPC = \frac{C_{A,T}}{CRF(r, m_p)} \quad (14)$$

$$CRF(r, m_p) = \frac{r(1+r)^{m_p}}{(1+r)^{m_p}-1} \quad (15)$$

where, m_p represents the lifespan of the entire HRE system as an economic project.

4.2 Loss of power supply probability

In the case of a grid-tied HRE system, penalties are incurred if the LPSP surpasses predetermined limits. In this study, LPSP is constrained not to exceed a predefined value ($LPSP_{Max}$ = 0.05), and its calculation follows the formula below [26]:

$$LPSP = \begin{cases} 0, & P_{Deficit}(t) \le P_{GP}^{Max} \\ \frac{\sum_{t=1}^{8760}[P_{Deficit}(t) - P_{GP}^{Max}]}{\sum_{t=1}^{8760} P_L(t)}, & else \end{cases} \quad (16)$$

4.3 Carbon emissions

The carbon emissions from an external grid (CE_{Grid}) are associated with the amount of purchased electricity from the utility grid, and this relationship can be represented as follows [27]:

$$CE_{Grid} = \sum_{t=1}^{8760} P_{GP}(t) \cdot EF_{Grid} \quad (17)$$

where EF_{Grid} denotes the emission factor of the external grid, which is set to 0.632 kg/kWh [28].

4.4 Objective function

In this study, the objective function for the optimization algorithm is introduced, aiming to minimize the COE, LPSP, and CE_{Grid}. This objective function can be defined as follows:

$$min\ OF = \min(\lambda_1 \cdot COE + \lambda_2 \cdot CE_{Grid} + \lambda_3 \cdot LPSP) \quad (18)$$

The AVOA optimizer has been employed to determine the optimal design of the suggested HRE system while adhering to the following constraints:

$$LPSP \le 0.05 \quad (19)$$

$$P_{GP}(t) \le P_{GP}(Max) \quad (20)$$

$$P_{GS}(t) \le P_{GS}(Max) \quad (21)$$

4.5 African vultures optimization algorithm

The AVOA, a novel nature-inspired metaheuristic algorithm, was introduced in 2021 [29]. This algorithm was created by simulating the natural behaviors and foraging habits of African vultures. African vultures can be categorized into three groups based on their unique physical traits. The first group comprises vultures that are physically stronger and have a higher likelihood of obtaining food compared to other vultures. The second group of vultures is characterized by physical weakness compared to the first group, while the third group consists of vultures with even lower physical strength than those in the first two groups. When searching for food, vultures tend to gather around the group that has found a food source, potentially leading to multiple vulture species competing for the same food. Less dominant vultures form circles around stronger ones and consume food by exhausting them, while starving vultures may exhibit increased aggression. The mathematical formulas employed for the AVOA in this research article correspond to those outlined in the work of [29].

5 Results and Discussion

To assess the benefits of the suggested optimizer, an actual case study was conducted to size an HRE system. The chosen case study took place in Zafarana, Egypt. Zafarana, situated at latitude 29.115 and longitude 32.658, is a coastal region in Egypt positioned on the western

shores of the Red Sea. It is approximately 200 kilometers southeast of Cairo. Zafarana benefits from abundant sunshine for the majority of the year, and the average wind speed remains at 8 m/s throughout the year. The monthly data for wind speeds and horizontal solar radiation throughout the year in the Zafarana site were obtained from the NASA website as shown in Fig. 3 [30]. Figure 4 displays the average monthly load curve for the region being studied. The technical specifications and costs of the components for the HRE system are provided in Table 1 [31].

Table 1. Input data [31].

Component	Parameter	Value	Unit
PVS	Model	PV – MLT260HC	
	$P_{R,PV}$	260	W
	T_{nom}	25	°C
	σ_T	0.004	1/°C
	r_{nom}	1000	W/m2
	Initial cost	112	$/unit
	Maintenance cost	1%	
	Lifespan	25	Years
WT	Model	Fuhrländer FL 30	
	$P_{R,WT}$	30	kW
	w_R	12	$/unit
	$w_{c,i}$	2.5	$/unit
	$w_{c,o}$	25	$/unit
	Initial cost	58,564.79	$/unit
	Maintenance cost	3%	
	Lifespan	20	Years
Battery	Model	RS lead acid battery	
	Size	12V(50Ah)	
	μ_B	0.002	
	η_C	90%	
	η_D	85%	
	Initial cost	146.5	$/unit
	Maintenance cost	3%	
	Lifespan	10	Years
Converter	η_{conv}	95%	
	Initial cost	711	$/kW
	Lifespan	10	
Others	m_p	25	Years
	r	6%	

The MATLAB software was employed to achieve the results, with a maximum of 100 iterations and a maximum of 30 search agents being utilized for both optimizers to ensure a fair comparison between AVOA and PSO.

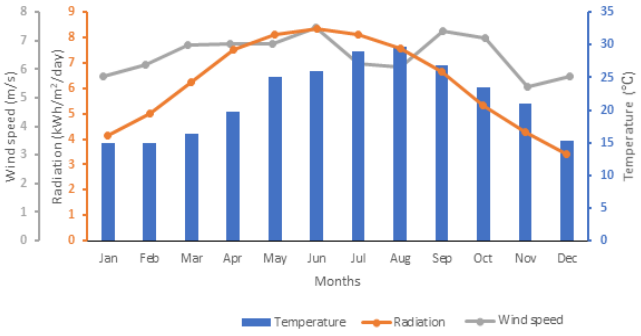

Fig. 3. Weather data of Zafarana.

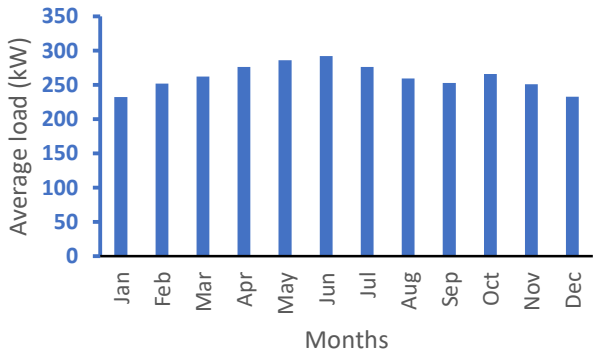

Fig. 4. The average monthly load demand.

The optimizer proposed in this study incorporates multiple objectives aimed at minimizing costs, enhancing reliability, and reducing CO_2 emissions from the HRE system. This optimization is performed using hourly available data. In this work, the design of the proposed HRE system is determined by the respective numbers of PV panels, wind turbines, and batteries. The convergence curves of the AVOA and PSO, spanning 100 iterations, is depicted in Fig. 5. Table 2 displays the optimal sizing outcomes of AVOA and PSO for the HRE system consisting of PV panels, WTs, and batteries, which are connected to the grid. The results show that the AVOA optimization approach can capable to reach the minimum best optimal value of the objective function. Based on the AVOA optimizer results, the recommended configuration to achieve the lowest COE of 0.0901 $/kWh at the specified site includes 2000 PV units, 20 WTs, and 192 batteries.

Table 2. Optimization outcomes of the proposed HRE system.

Characteristics	AVOA	PSO
Best objective function	0.0709	0.070926
$n_{PV,Panels}$	2000	1923
n_{WTs}	20	20
No. of batteries	192	202
Purchased from grid(kWh/year)	551,548	556,372.9
Sold to grid (kWh/year)	687,686.5	654,154.7
COE ($/kWh)	0.0901	0.0929
NPC ($)	2,639,493	2,720,644
LPSP	$2.7722*10^{-11}$	0.001
CO_2 emissions (kg/year)	348,578	351,628

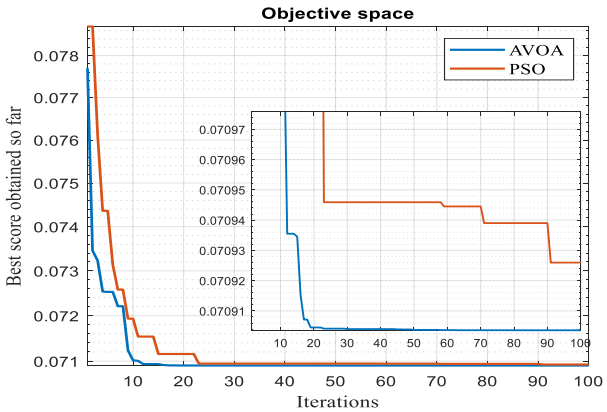

Fig. 5. Convergence curves of AVOA and PSO.

This outcome corresponds to an NPC of 2.6395 million $ and guarantees a LPSP value of 2.7722e-11, which matches the specified value (<0.05). Furthermore, the estimated yearly carbon emissions amount to 348,578 kg. According to the data presented in Fig. 6, the energy production breakdown is 47% from WTs, 35% from PVS, and the remaining 18% is obtained through purchasing from the electric grid. On the other hand, 77% of the total energy consumption is utilized to meet load demand, while the remaining 23% is sold back to the grid.

Figure 7 illustrates the change in power produced each hour for the different components of the HRE system at the optimal solution. Figure 8 displays the simulation results for a specific day (24 h), showcasing the performance of the HRE based on the optimal sizing obtained from the AVOA algorithm. Considering the sizing constraints, it is challenging to meet the optimization requirements while maintaining zero power exchange with the utility grid. The figure clearly illustrates that there is a significant amount of time where electricity flows to and from the grid in order to meet the load demand. During the hours when renewable systems produce a high amount of electricity, the surplus power is primarily utilized to recharge the batteries. Any remaining excess energy is then sold to the external grid. During periods when the generation from the HRE system decreases, the first priority is to meet the load demand by utilizing the energy stored in the batteries. If there is still a deficit, the remaining energy needed is obtained from the grid through purchasing.

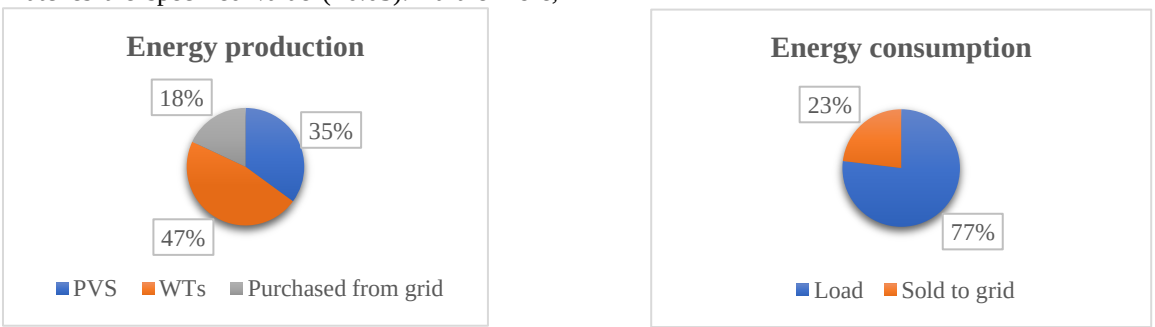

Fig. 6. An overview of AVOA results for annual energy production and consumption percentages.

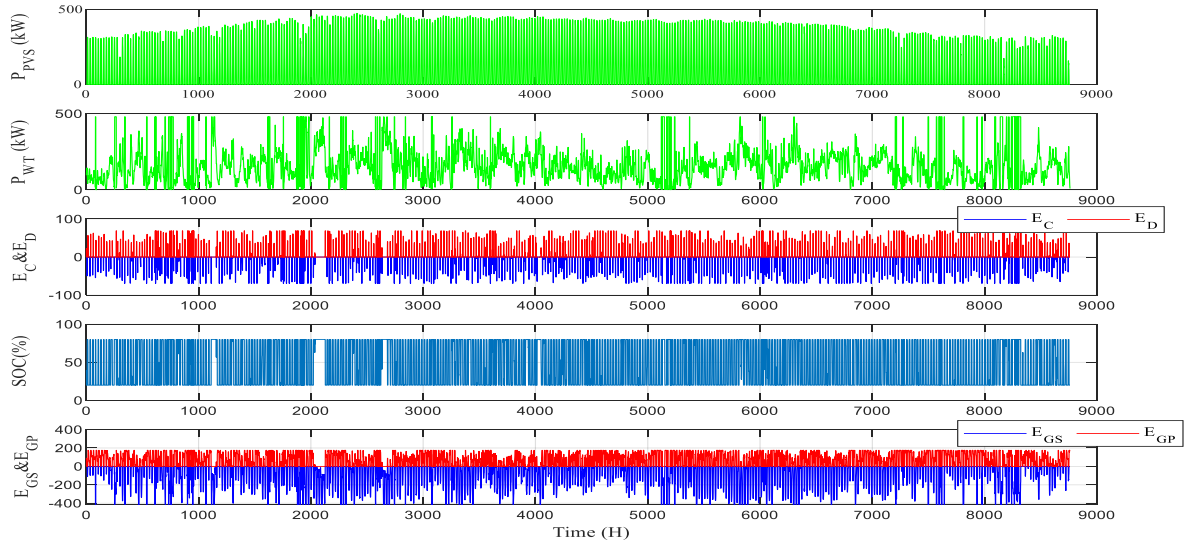

Fig. 7. AVOA algorithm results for the optimal solution.

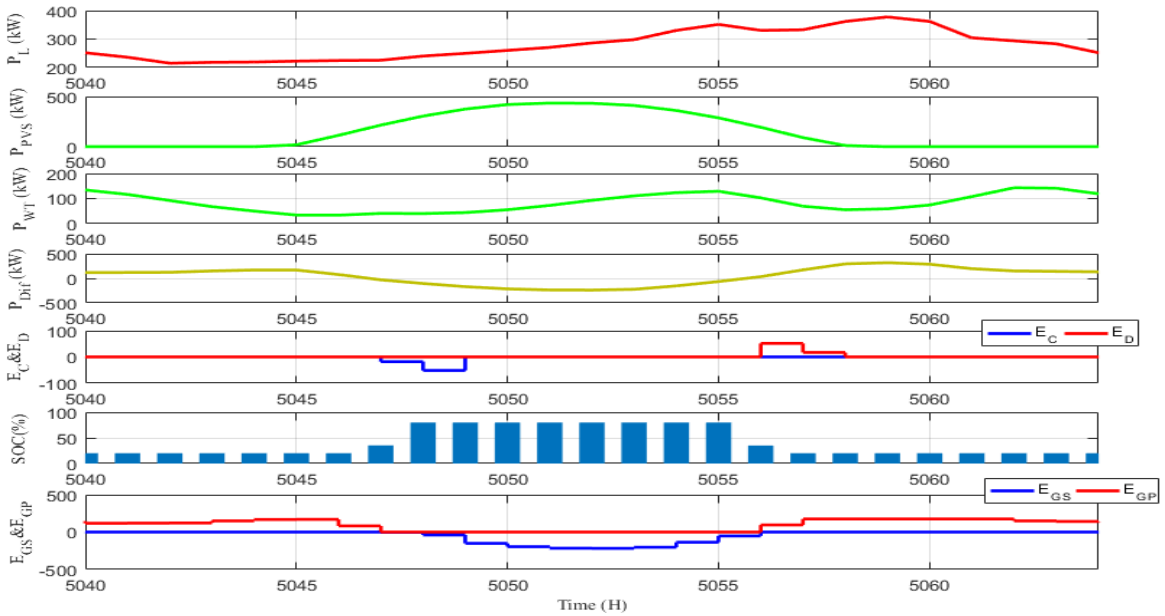

Fig. 8. Simulation results with AVOA for one day of operation.

6 Conclusion

In this study, the AVOA is implemented in MATLAB to achieve the optimal design of a grid-dependent HRE system in Zafarana, Egypt. The primary objective of this research is to meet the load demand of the specified location while minimizing COE, ensuring the lowest level of LPSP, and minimizing CO_2 emissions. A comparative analysis between AVOA and PSO is provided, showing AVOA's superior operational efficiency, particularly in terms of COE and convergence speed. The optimization outcomes demonstrate that the AVOA optimizer has successfully achieved the best value for the objective function, which corresponds to a minimum COE of 0.0901 $/kWh. The optimization results yield an NPC of 2.6395 million dollars and an LPSP value of 2.7722e-11, meeting the specified requirement of being less than 0.05. Additionally, the annual carbon emissions are estimated to be 348,578 kg. Future works could explore the incorporation of additional renewable energy sources and diverse energy storage technologies. Also, applying different types of demand response programs to enhance system reliability without necessitating an increase in the size of HRE system and, consequently, increase system cost.

References

[1] M. Goedecke, S. Therdthianwong, and S. H. Gheewala, "Life cycle cost analysis of alternative vehicles and fuels in Thailand," *Energy Policy*, vol. 35, no. 6, pp. 3236–3246, 2007, doi: 10.1016/j.enpol.2006.11.015.

[2] M. Abd El Sattar, W. A. Hafez, A. A. Elbaset, and A. H. K. Alaboudy, "Economic Valuation of Electrical Wind Energy in Egypt Based on Levelized Cost of Energy," *Int. J. Renew. Energy Res.*, vol. 10, no. 4, pp. 1888–1891, 2020, doi: 10.20508/ijrer.v10i4.11463.g8079.

[3] K. Kusakana and H. J. Vermaak, "Hybrid renewable power systems for mobile telephony base stations in developing countries," *Renew. Energy*, vol. 51, pp. 419–425, 2013, doi: 10.1016/j.renene.2012.09.045.

[4] S. A. Mohamed and M. Abd El Sattar, "A comparative study of P&O and INC maximum power point tracking techniques for grid-connected PV systems," *SN Appl. Sci.*, vol. 1, no. 2, pp. 1–13, 2019, doi: 10.1007/s42452-018-0134-4.

[5] M. Abdelsattar, I. Hamdan, A. Mesalam, and A. Fawzi, "An Overview of Smart Grid Technology Integration with Hybrid Energy Systems Based on Demand Response," in *2022 23rd International Middle East Power Systems Conference (MEPCON)*, IEEE, 2022, pp. 1–6.

[6] J. Zhou and Z. Xu, "Optimal sizing design and integrated cost-benefit assessment of stand-alone microgrid system with different energy storage employing chameleon swarm algorithm: A rural case in Northeast China," *Renew. Energy*, vol. 202, pp. 1110–1137, Jan. 2023, doi: 10.1016/j.renene.2022.12.005.

[7] N. Alshammari and J. Asumadu, "Optimum unit sizing of hybrid renewable energy system utilizing harmony search, Jaya and particle swarm optimization algorithms," *Sustain. Cities Soc.*, vol. 60, Sep. 2020, doi: 10.1016/j.scs.2020.102255.

[8] A. Maleki, "Optimization based on modified swarm intelligence techniques for a stand-alone hybrid photovoltaic/diesel/battery system," *Sustain. Energy Technol. Assessments*, vol. 51, Jun. 2022, doi: 10.1016/j.seta.2021.101856.

[9] M. M. Kamal, I. Ashraf, and E. Fernandez, "Optimal sizing of standalone rural microgrid for sustainable electrification with renewable energy resources," *Sustain. Cities Soc.*, vol. 88, Jan. 2023, doi: 10.1016/j.scs.2022.104298.

[10] M. M. Samy, H. I. Elkhouly, and S. Barakat, "Multi-objective optimization of hybrid renewable energy system based on biomass and fuel cells," *Int. J. Energy Res.*, vol. 45, no. 6, pp. 8214–8230, May 2021, doi: 10.1002/er.5815.

[11] S. M. Mahmoudi, A. Maleki, and D. Rezaei Ochbelagh, "Investigating the role of the carbon tax and loss of power supply probability in sizing a hybrid energy system, economically and environmentally," *Energy Convers. Manag.*, vol. 280, Mar. 2023, doi: 10.1016/j.enconman.2023.116793.

[12] M. M. Gamil, T. Senjyu, H. Takahashi, A. M. Hemeida, N. Krishna, and M. E. Lotfy, "Optimal multi-objective sizing of a residential microgrid in Egypt with different ToU demand response percentages," *Sustain. Cities Soc.*, vol. 75, 2021, doi: 10.1016/j.scs.2021.103293.

[13] M. A. Mohamed, A. M. Eltamaly, A. I. Alolah, and A. Y. Hatata, "A novel framework-based cuckoo search algorithm for sizing and optimization of grid-independent hybrid renewable energy systems," *Int. J. Green Energy*, vol. 16, no. 1, pp. 86–100, 2019, doi: 10.1080/15435075.2018.1533837.

[14] M. A. Mohamed, A. M. Eltamaly, and A. I. Alolah, "Swarm intelligence-based optimization of grid-dependent hybrid renewable energy systems," *Renew. Sustain. Energy Rev.*, vol. 77, no. February 2016, pp. 515–524, 2017, doi: 10.1016/j.rser.2017.04.048.

[15] M. A. Mohamed, A. M. Eltamaly, and A. I. Alolah, "PSO-based smart grid application for sizing and optimization of hybrid renewable energy systems," *PLoS One*, vol. 11, no. 8, pp. 1–22, 2016, doi: 10.1371/journal.pone.0159702.

[16] A. M. Eltamaly, M. A. Mohamed, and A. I. Alolah, "A novel smart grid theory for optimal sizing of hybrid renewable energy systems," *Sol. Energy*, vol. 124, pp. 26–38, 2016, doi: 10.1016/j.solener.2015.11.016.

[17] A. Naderipour, A. R. Ramtin, A. Abdullah, M. H. Marzbali, S. A. Nowdeh, and H. Kamyab, "Hybrid energy system optimization with battery storage for remote area application considering loss of energy probability and economic analysis," *Energy*, vol. 239, Jan. 2022, doi: 10.1016/j.energy.2021.122303.

[18] A. A. Z. Diab, H. M. Sultan, and O. N. Kuznetsov, "Optimal sizing of hybrid solar/wind/hydroelectric pumped storage energy system in Egypt based on different meta-heuristic techniques", Environmental Science and Pollution Research, vol. 27, pp. 32318-32340, 2020, doi: 10.1007/s11356-019-06566-0.

[19] F. S. Mahmoud *et al.*, "Optimal sizing of smart hybrid renewable energy system using different optimization algorithms," *Energy Reports*, vol. 8, pp. 4935–4956, 2022, doi: 10.1016/j.egyr.2022.03.197.

[20] R. Khezri, A. Mahmoudi, and M. H. Haque, "Optimal Capacity of Solar PV and Battery Storage for Australian Grid-Connected Households," *IEEE Trans. Ind. Appl.*, vol. 56, no. 5, pp. 5319–5329, 2020, doi: 10.1109/TIA.2020.2998668.

[21] H. Demolli, A. S. Dokuz, A. Ecemis, and M. Gokcek, "Location-based optimal sizing of hybrid renewable energy systems using deterministic and heuristic algorithms," *Int. J. Energy Res.*, vol. 45, no. 11, pp. 16155–16175, Sep. 2021, doi: 10.1002/er.6849.

[22] A. A. Zaki Diab, S. I. El-Ajmi, H. M. Sultan, and Y. B. Hassan, “Modified farmland fertility optimization algorithm for optimal design of a grid-connected hybrid renewable energy system with fuel cell storage: Case study of Ataka, Egypt,” *Int. J. Adv. Comput. Sci. Appl.*, vol. 10, no. 8, pp. 119–132, 2019.

[23] S. Singh and S. C. Kaushik, “Optimal sizing of grid integrated hybrid PV-biomass energy system using artificial bee colony algorithm,” *IET Renew. Power Gener.*, vol. 10, no. 5, pp. 642–650, 2016, doi: 10.1049/iet-rpg.2015.0298.

[24] F. S. Mahmoud, A. M. Abdelhamid, A. Al Sumaiti, A. H. M. El-Sayed, and A. A. Z. Diab, “Sizing and Design of a PV-Wind-Fuel Cell Storage System Integrated into a Grid Considering the Uncertainty of Load Demand Using the Marine Predators Algorithm,” *Mathematics*, vol. 10, no. 19, 2022, doi: 10.3390/math10193708.

[25] M. M. M. Islam *et al.*, “Techno-economic Analysis of Hybrid Renewable Energy System for Healthcare Centre in Northwest Bangladesh,” *Process Integration and Optimization for Sustainability*, vol. 7, no. 1–2. pp. 315–328, 2023. doi: 10.1007/s41660-022-00294-8.

[26] S. Singh, P. Chauhan, and N. J. Singh, “Capacity optimization of grid connected solar/fuel cell energy system using hybrid ABC-PSO algorithm,” *Int. J. Hydrogen Energy*, vol. 45, no. 16, pp. 10070–10088, Mar. 2020, doi: 10.1016/j.ijhydene.2020.02.018.

[27] O. Nadjemi, T. Nacer, A. Hamidat, and H. Salhi, “Optimal hybrid PV/wind energy system sizing: Application of cuckoo search algorithm for Algerian dairy farms,” *Renew. Sustain. Energy Rev.*, vol. 70, pp. 1352–1365, 2017, doi: 10.1016/j.rser.2016.12.038.

[28] S. Barakat, M. M. Samy, M. B. Eteiba, and W. I. Wahba, “Feasibility Study of Grid Connected PV-Biomass Integrated Energy System in Egypt,” *Int. J. Emerg. Electr. Power Syst.*, vol. 17, no. 5, pp. 519–528, 2016, doi: 10.1515/ijeeps-2016-0056.

[29] B. Abdollahzadeh, F. S. Gharehchopogh, and S. Mirjalili, “African vultures optimization algorithm: A new nature-inspired metaheuristic algorithm for global optimization problems,” *Comput. Ind. Eng.*, vol. 158, no. 107408, 2021, doi: , doi: 10.1515/ijeeps-2016-0056.

[30] “NASA POWER.” https://power.larc.nasa.gov/data-access-viewer/ (accessed Sep. 15, 2023).

[31] A. A. Zaki Diab, H. M. Sultan, I. S. Mohamed, N. Kuznetsov Oleg, and T. D. Do, “Application of different optimization algorithms for optimal sizing of pv/wind/diesel/battery storage stand-alone hybrid microgrid,” *IEEE Access*, vol. 7, pp. 119223–119245, 2019, doi: 10.1109/ACCESS.2019.2936656.